A Family of Carbon-Based Nanocomposite Tubular Structures Created by *in Situ* Electron Beam Irradiation

Jian-Wei Liu,[†] Jie Xu,[†] Yong Ni,[‡] Feng-Jia Fan,[†] Chuan-Ling Zhang,[†] and Shu-Hong Yu[†,*]

[†]Division of Nanomaterials & Chemistry, Hefei National Laboratory for Physical Sciences at Microscale, Department of Chemistry, National Synchrotron Radiation Laboratory, University of Science and Technology of China, Hefei 230026, P. R. China, and [‡]CAS Key Laboratory of Mechanical Behavior and Design of Materials, University of Science and Technology of China, Hefei 230026, P. R. China

ABSTRACT

We report a unique approach for the fabrication of a family of curling tubular nanostructures rapidly created by a rolling up of carbon membranes under *in situ* TEM electron beam irradiation. Multiwall tubes can also be created if irradiation by electron beam is performed long enough. This general approach can be extended to curve the conductive carbon film loaded with various functional nanomaterials, such as nanocrystals, nanorods, nanowires, and nanosheets, providing a unique strategy to make composite tubular structures and composite materials by a combination of desired optical, electronic, and magnetic properties, which could find potential applications, including fluid transportation, encapsulation, and capillarity on the nanometer scale.

KEYWORDS: *in situ* TEM · electron beam irradiation · curling · tubular nanostructures · nanocomposite

Nanofabrication and self-assembly of nanobuilding blocks have become one of the most active research areas in materials science.[1−4] Many kinds of nanostructures have been successfully achieved by self-assembly or directed assembly. Multicomponent assembly provides a route to unique combination of desired optical, electronic, and magnetic properties that are often not available in single-component materials.[5−9]

Self-assembly processes can be initiated by various stimuli, including directed by small molecules,[10,11] extra force,[12−15] phase interface,[12−16] evaporation of solvent,[17,18] and the color and intensity of incident light,[19,20] photochemistry triggered,[21,22] electron-beam irradiation.[23] Irradiation can lead to a situation where the solid is far from thermal equilibrium and, under certain circumstances which leads to direct interactions between incident electrons and materials, can fulfill the condition for the formation of self-assembled structures.[24,25] Transmission electron microscopy (TEM) is undoubtedly one of the most useful tools that is not only used for the investigation of nanostructures of all kinds, but also has the advantage that structural alteration of the specimen by electron irradiation can be severe and lead to the formation of unexpected and very exciting structures.[26,27] Despite the enormous success we have made so far, nanofabrication and assembly of nanosized building blocks are still difficult and lack a sufficient level of control and there exists a strong need for further development.[28]

Herein, we directly assemble nanosized building blocks, such as nanoparticles, nanorods, nanowires, and nanosheet monolayers loaded on conductive carbon film with a thickness of about 10 nm into tubular structures driven by *in situ* electron-beam irradiation. A wide range of possible materials can be engineered to produce carbon-based tubular structures in this way, making these tubes suitable candidates for use in fundamental research as well as in applications. To investigate the capability of the *in situ* rolling process, single Ag nanowire, disordered Ag nanowires with low density, and ordered Ag nanowire film fabricated by the Langmuir-Blodgett (LB) technique were selected as the elastic metal objects with structural memory to store mechanical energy for their potential applications.

* Address correspondence to shyu@ustc.edu.cn.

Received for review March 24, 2012 and accepted April 24, 2012.

Published online April 24, 2012
10.1021/nn301310m

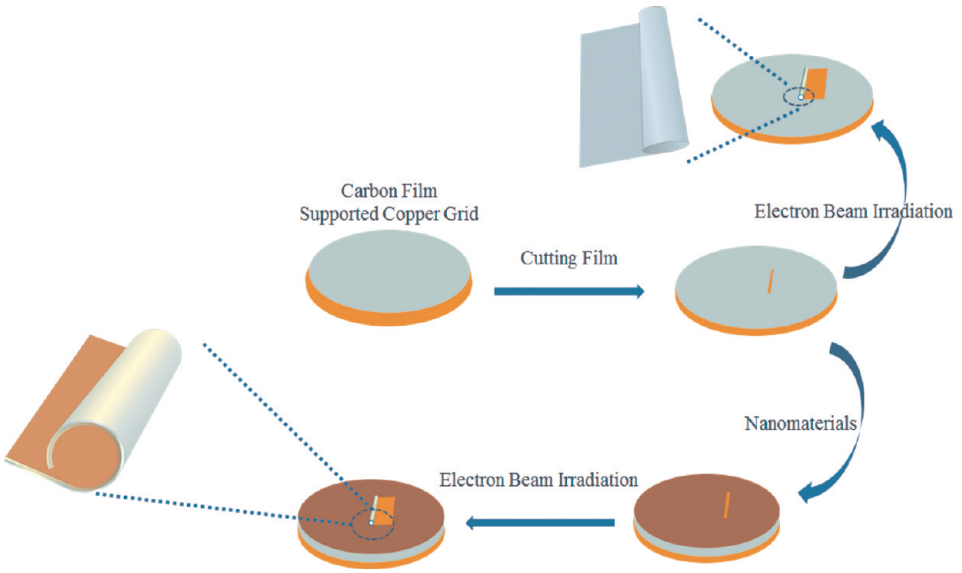

Figure 1. Schematic illustration of carbon-based solid films rolled up into nanotubes under the electron-beam irradiation.

RESULTS AND DISCUSSION

Four kinds of nanocrystals with different dimensionalities, that is, nanoparticles, nanorods, nanowires, and nanosheets were chosen to demonstrate the versatility of the present strategy. Synthetic recipes of Cu_2ZnSnS_4 nanocrystals,[29] Au nanorods,[30] Ag nanowires,[31] and uniform Te nanowires have been described previously.[32] 2D monolayers of oxide graphite have been also synthesized from natural graphite (SP-1) by modified methods described previously.[33−35]

In the present case, *in situ* formation of nanotubes, with diameters of hundreds nanometers and length of tens of micrometers, can be achieved by electron beam irradiation which can be carried out on a commercial JEOL-7650 transmission electron microscope operated at an accelerating voltage of 100 kV.

As shown in Figure 1, first, a common TEM Cu grid (300 mesh) (see Supporting Information, Figure S1) supported by carbon film with a thickness of 10 nm was used here without further pretreatment or functionalization.[36] After a slit was introduced into the sample surface and the structure was exposed to irradiation by an electron beam, it was observed to first begin to bend up into a nearly cylindrical surface due to strain relief and then roll up to nanotubes gradually. In addition, when the nanosized building blocks, such as nanoparticles, nanorods, nanowires, and nanosheet monolayers were loaded onto the carbon film supported side of TEM grid, respectively, they can coroll up with the carbon film driven by electron-beam irradiation. The bottom carbon-based film is supposed to provide the necessary strain to force the roll-up of the nanomaterials membrane which then assumes a cylindrical shape.

Figure 2 shows the observed time-dependent TEM images of carbon films curling with time prolonging at 100 kV after the time interval of 1 s (Figure 2a−d). If irradiation by electron beam is performed long enough, multiwall tubes can be created as shown in Figure 2d. It will curl more slowly when the nanosized building blocks are added on to the carbon film, so we can show the progress with more details. The size and shape of the carbon membrane slit are the most important influencing factors in controlling the diameter of the tubular structures (Figure 3). Besides this, there are many factors related to the diameter of the tubular structures such as the working voltage, current density, and extra nanomaterials that are introduced.

Figure 4 shows a series of time dependent TEM images of ultrathin Te nanowires loaded on carbon films curling with time prolonging at 100 kV, after the same time interval of 5 s (Figure 4a−d). The solid film began to roll up when the electron was focused on. Since the rolling takes place in the detaching area of the substrate, the process is readily compatible with some nature system. An analogous transformation process is found in biology, where the interaction of membrane molecules modifies the lateral tension of a lipid bilayer. Five seconds later in Figure 4a, more remarkable curvature and, in particular, the tubular structures are formed (Figures 4c and 4d). If the irradiation time is enough, nanowire-based tubes are created. Just like any other emerging research frontier, researchers working in the nanowire assembly field try to develop new complicated structures to expand expected applications. As a general and versatile assembly method, this *in situ* electron beam irradiation induced tube formation strategy reported here can be extended to roll up many other kinds of nanosized building blocks with different dimensionalities, such as nanoparticles, nanorods, and nanosheets.

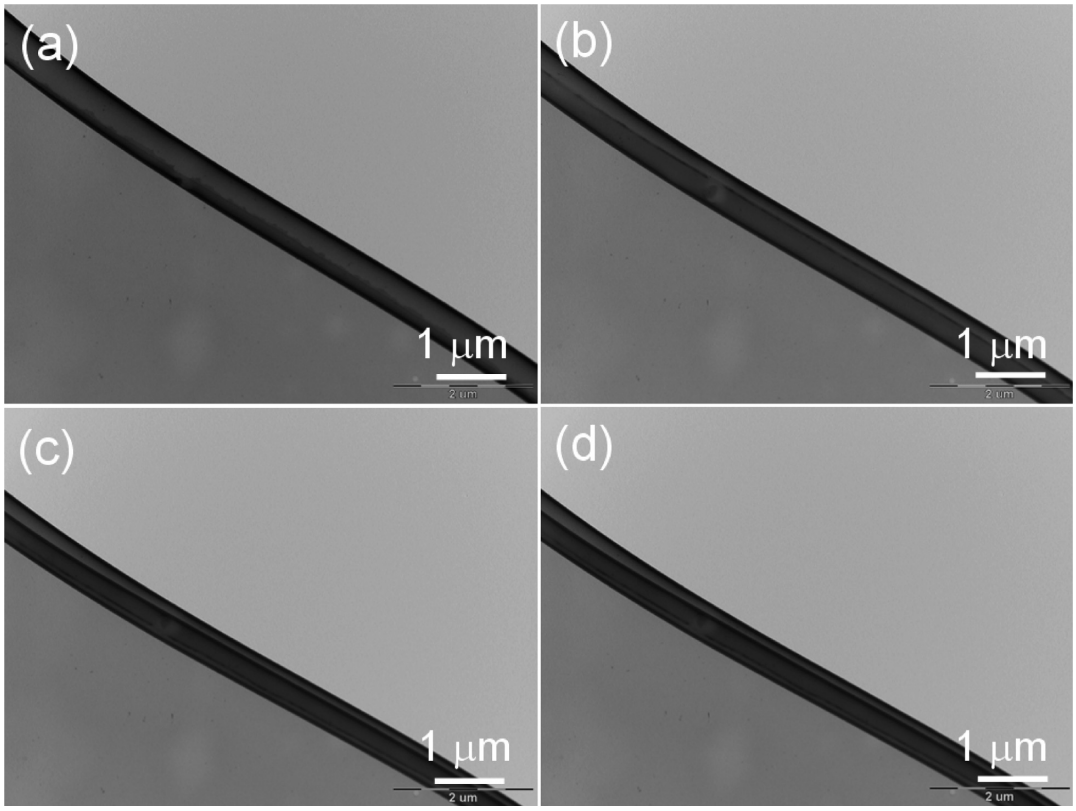

Figure 2. Carbon film curling (a–d) with time going on under the electron-beam irradiation of TEM at 100 kV. The time interval is 1 s.

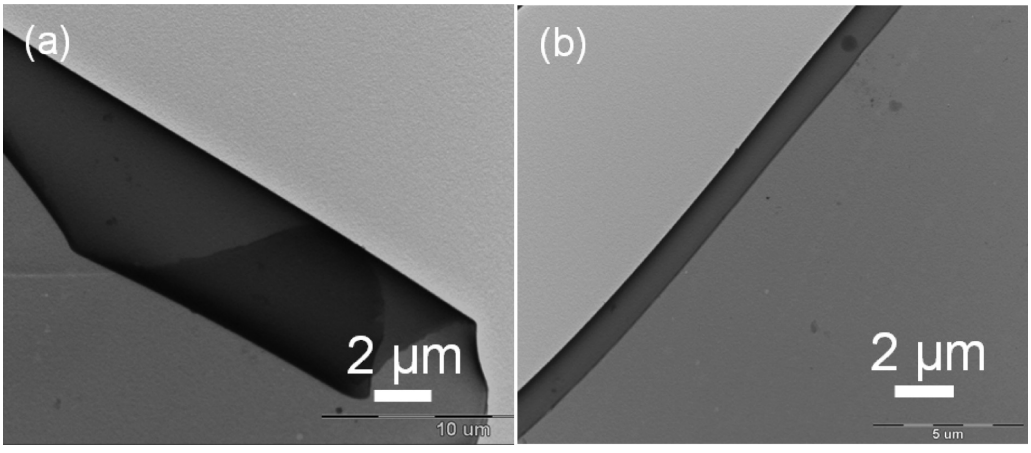

Figure 3. (a, b) TEM images of the curled carbon film tubes formed with the membrane slits of different size and shape.

Zero dimension nanoparticles with a diameter of 10 nm, nanorods with a diameter of width 19 nm and a length of 78 nm, and two dimension nanosheets (*e.g.*, graphene) can be coassembled driven by electron beam irradiation, respectively (Figure 5a–c). The nanosized building blocks were synthesized based on previous reported recipes (see Supporting Information, Experimental Section). The obtained products were confirmed by analysis of X-ray diffraction, UV–vis absorption spectra, and Raman spectroscopy (see Supporting Information, Figures S2–S6).

The conversion of kinetic and elastic potential energy is of critical significance for device fabrication to achieve novel functions. Rigid Ag nanowires as the elastic metal objects with structural memory were introduced here to store mechanical energy for their potential applications. First, Ag nanowires were synthesized and confirmed by X-ray diffraction (see Supporting Information, Figure S7). To investigate the power of the *in situ* rolling process, single Ag, disordered Ag nanowires with low density, and ordered Ag nanowire film fabricated by LB technique[37] were

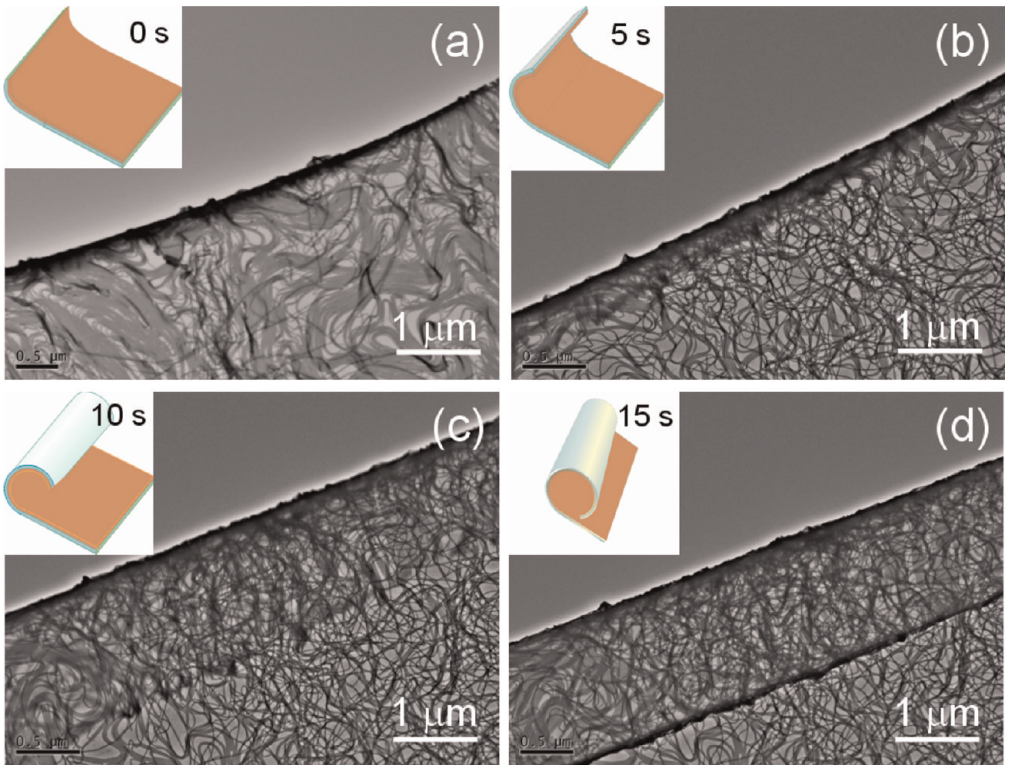

Figure 4. (a–d) Time-dependent cocurling assembly of a carbon film with nanowires under the irradiation of a TEM beam at 100 kV. The time interval for panels a, b, c, and d is 5 s. The insets illustrated the irradiation time-dependent curing states of the ultrathin Te nanowires with a high aspect ratio.

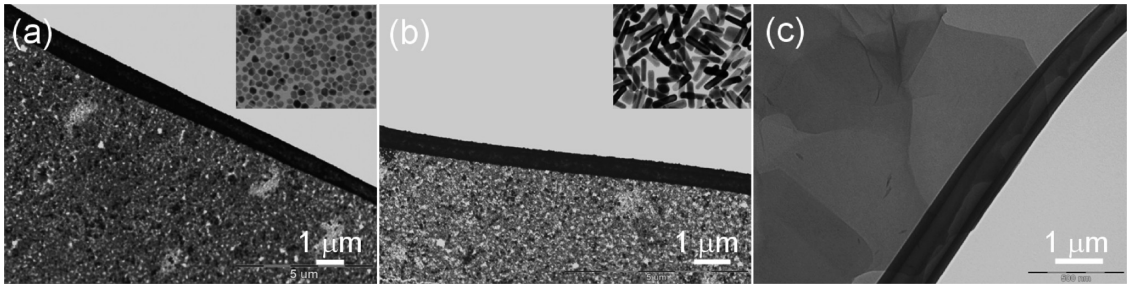

Figure 5. (a–c) Carbon film curling with monodisperse Cu_2ZnSnS_4 nanoparticles, Au nanorods, and graphene. The insets in panels a and b show the magnified images of nanoparticles and nanorods loaded on the carbon film in panels a and b, respectively.

added onto the carbon film supported-side of TEM grid with a slit. The samples were then exposed to irradiation by an electron beam of TEM. It was observed that a single Ag nanowire was curving rapidly as shown in Figure 6a–c; the time interval is 5 s. Compared with flexible ultrathin Te nanowires, Ag nanowires with a diameter of 60 nm, and length of 15 μm used here were rigid.[31] From Figure 6 panels d to f, the time interval is 10 s, indicating the rolling process becomes more difficult. With the nanowire density increasing as shown in Figure 5g, the situation is more complicated. Ordered Ag nanowires obtained by the LB technique (Figure 6g) can be curled with carbon film from the lateral direction, but are unaffected from the axial direction (Figure 6h,i).

To take advantage of this type of tubular building blocks, understanding the mechanisms of rolling process is essential.[38,39] A system far from equilibrium can exhibit complex transitory structures, and curly structures can be formed from thin solid films when they are freed from a substrate, and once released from their substrate the layer rolls up by itself and forms a nanotube.[40–45] In 1909, Stoney reported that strained metal layers spontaneously "curl up into beautiful close rolls" once they detach from their host substrate.[46] Currently, there are two methods for preparing these solid state nanotubes, involving a general and a specialized procedure.[40] Both rely on the release of thin layers from a substrate. For the general method, a thin solid film with almost arbitrary composition is detached from its substrate and folded back onto its own surface. The resultant crease forms a nanotube. The specialized method relies on inherently built in

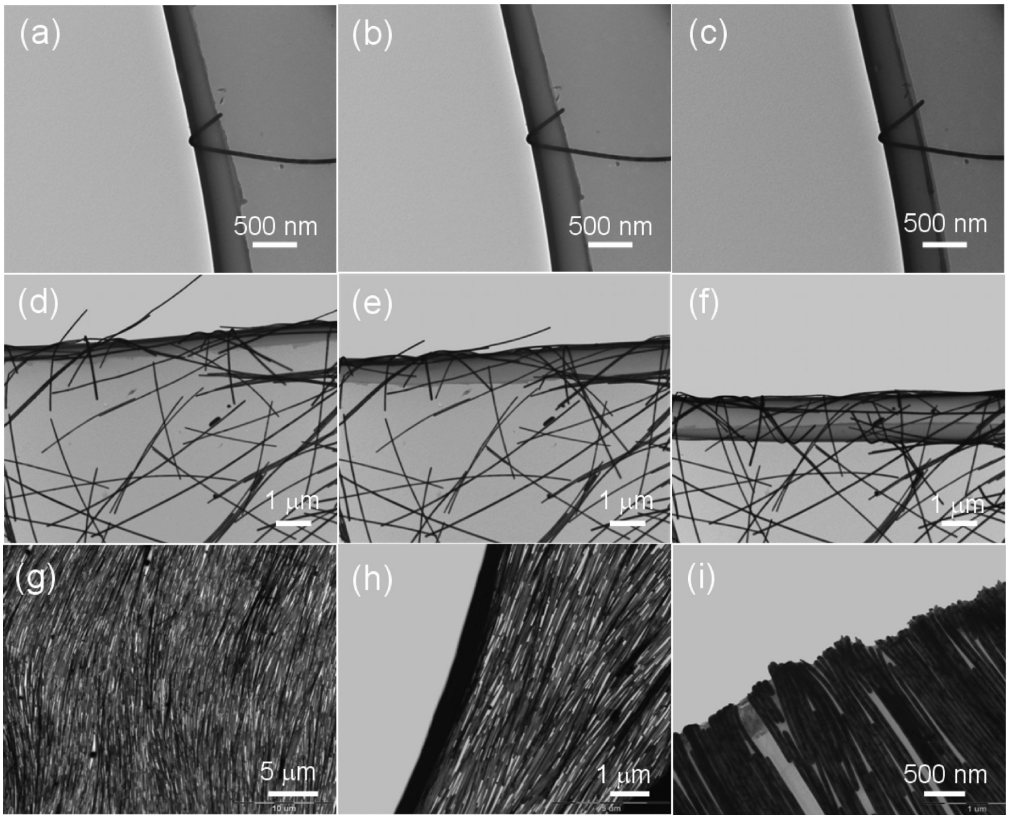

Figure 6. (a–c) Time-dependent TEM images of cocurling of carbon film with a single Ag nanowire, with time prolonging under the electron-beam irradiation of TEM equipment at 100 kV. The time interval for panels a–c is 5 s. (d–f) Time-dependent TEM images of cocurling of carbon film with disordered Ag nanowires with lower density under the electron beam irradiation of TEM equipment at 100 kV. The time interval for panels d–f is 10 s. (g) Ordered Ag nanowires assembled by LB with higher density. (h) TEM images of carbon film can curl with ordered Ag nanowires from the lateral direction, but cannot curl from axial direction (i).

strain within the thin solid film. Once the film is freed from the substrate, the layer rolls up by itself and forms a nanotube.

It is well established that mismatch strain between different layers in thin film systems can induce mechanical deformation either in the form of surface waviness formation or in the form of bending and rolling of thin membranes. When two mismatched epitaxial layers are constrained to a substrate, a tremendous amount of residual strain energy is stored in the bilayer membrane. Once it is released from the constraint of the substrate, the membrane relieves the stored strain energy by rolling up to form various 3D structures including micro- and nanotubes. Irradiation effects in carbon nanostructures have been investigated previously.[43,47,48] Ugarte reported graphitic networks showed curling and closure under electron beam irradiation in 1992.[49] The temperature of the top of the carbon film differs from the bottom under TEM electron irradiation, providing the necessary strain to force the roll-up of the nanomembrane which then assumes a cylindrical shape.

If we assume that the formation of the hybrid tubular structure is the result of optimal release of the elastic energy stored in the carbon films induced by the electron beam irradiation, the curvature of the rolled-up tubular structures can be estimated by the model of multilayer hinged structures with residual strains.[50] For a bilayer film, it consists of bottom and top layers with thickness h_1 and h_2, which are subject to biaxial residual strain ε_1 and ε_2, with respect to the substrate, respectively. The detaching area of the substrate is characterized by $W \times L$ with W and L being the etching length and the width of the slit, respectively. The radius of the tubular structure can be written as

$$R = \frac{h_1[1+\beta^2\alpha^4+2\beta\alpha(2+2\alpha^2+3\alpha)]}{6\eta\beta\alpha(1+\alpha)(\varepsilon_2-\varepsilon_1)} \quad (1)$$

where $\alpha = h_2/h_1$, $\beta = E_2'/E_1'$ with $E' = E/(1-v)^2$, and η is a shape factor as a function of L. $\eta = 1$ when L is small corresponding to the case of plane stress, and $\eta = 1 + v$ when L is large corresponding to the case of plane strain. The value of η can be determined through finite element simulation between the two cases. The result of eq 1 shows that we need to allow $\varepsilon_2 - \varepsilon_1 > 0$ such that the layer is rolled-up. In addition, we can control the radius of the tube by regulating the values of α and β through the hybrid process. It should be noted that the bilayer tends to wrinkle when it is totally compressed ($\varepsilon_2 < 0$, $\varepsilon_1 < 0$). The calculated result in

the reference[51] shows that a large value of W and L and a small value of $\varepsilon_2 - \varepsilon_1$ favor the wrinkle. We need to carefully control the dethatching process and try to avoid wrinkle toward the formation of a tubular structure.

CONCLUSION

In summary, we have successfully taken advantage of electron-beam-induced surface stress to directly and specifically roll up the carbon films into tubular structures, which are loaded with different nanostructures, such as nanoparticles, nanorods, nanowires, and nanosheets. This strategy has been demonstrated to be a general way, by which various nanomaterials with different shape and sizes can coassembly with the conductive carbon film and can be curved into tubular structures. Because various nanoparticles with different dimensionalities can be loaded on the TEM carbon film, this exceptional design flexibility is expected to fabricate different tubular structures and composite materials with promising applications, including fluid transportation, encapsulation, and capillarity on the nanometer scale.

METHODS

All reagents are of analytical grade and used without further purification.

Synthesis of Te Nanowires. All chemicals are of analytical grade and used as received without further purification. The synthesis of uniform Te nanowires was described previously.[32] In the typical synthesis, 1.0000 g of poly(vinyl pyrrolidone) (PVP, Shanghai Reagent Company, $M_W \approx 40\,000$) and 0.0922 g of Na_2TeO_3 were mixed with 33 mL of double distilled water into a 50 mL Teflon-lined stainless steel autoclave under vigorous magnetic stirring to form a homogeneous solution at room temperature. Then, 1.67 mL of hydrazine hydrate (85 wt %) and 3.33 mL of aqueous ammonia solution (25−28 wt %) were added into the mixed solution, respectively, under vigorous magnetic stirring for 5 min. The container was closed and maintained at 180 °C for 3 h. After that, the autoclave was cooled to room temperature naturally.

Synthesis of Au nanorods. Uniform Au nanorods were grown using the seed-mediated growth process described previously.[30] In a typical synthesis, a freshly prepared aqueous $NaBH_4$ solution (0.6 mL, 0.01 M) was added into an aqueous mixture solution made of $HAuCl_4$ (0.25 mL, 0.01 M) and CTAB (9.75 mL, 0.1 M). The resultant solution was mixed by rapid inversion for 2 min and then kept at room temperature undisturbed for at least 2 h. Then, $HAuCl_4$ (30 mL, 0.01 M), $AgNO_3$ (6 mL, 0.01 M), and CTAB (600 mL, 0.1 M) were mixed together. A freshly prepared aqueous ascorbic acid solution (4.8 mL, 0.1 M) was added, and the solution changed from yellow to colorless, which was followed by the addition of an aqueous HCl solution (12 mL, 1.0 M). After the resultant solution was mixed by inversion, the seed solution (1.44 mL) was added to the growth solution. The reaction mixture was subjected to gentle inversion for 10 s and then left undisturbed for at least 6 h.

Synthesis of Graphene Nanosheets. Graphene oxide was synthesized from natural graphite (SP-1) by modified methods described previously.[34] In a typical synthesis, 12 g of graphite powder, 10 g of $K_2S_2O_8$, and 10 g of P_2O_5 were added to 50 mL of concentrated H_2SO_4 solution at the temperature of 80 °C for 6 h. After that, the solution was diluted with 2 L of water, filtered, and washed using a 0.2 μm Nylon Millipore filter and dried in air overnight. For the following oxidation step, 460 mL of H_2SO_4 were chilled to 0 °C using an ice bath. The oxidized graphite was added to the acid and stirred. Then, 60 g of $KMnO_4$ were added slowly with temperature controlled below 10 °C. This mixture was allowed to react at 35 °C for 2 h, after which 920 mL of distilled water were added slowly to keep the temperature below 50 °C. After further reaction for 2 h, 2.8 L of water and 50 mL of 30% H_2O_2 were added, resulting in a brilliant yellow color along with bubbling. The mixture was allowed to fully settle for a few days before the supernatant was decanted. The remaining product was then filtered and washed with about 5 L of 10% HCl solution followed by 5 L of water to remove the acid. Finally, the product was dried in a vacuum at 60 °C for 6 h.

Synthesis of Silver Nanowires. Uniform Ag nanowires were prepared by the polyol process method reported previously.[31] In a typical synthesis, 5.86 g of PVP were added into 190 mL of glycerol into a 500 mL round bottle flask. After the formation of a homogeneous solution, 1.58 g of silver nitrate powder was added into the solution. Then 59 of mg NaCl and 0.5 mL of H_2O were added to 10 mL of glycerol solution. The flask was then immersed into a heating mantle equipped with a PTFE paddle stirrer. The solution temperature was raised from room temperature to 210 °C by gentle stirring (50 rpm) in 20 min. The color of the solution turned from pale white into light brown, red, dark gray, and eventually gray-green, indicating the nanowires formation. When the temperature reached 210 °C, the temperature was allowed to naturally cool. After that, water was added into the solution in 1: 1 ratio, and the mixture was centrifuged.

Assembly of Silver Nanowires by Langmuir−Blodgett Technique. The ordered AgNW monolayer was prepared at room temperature using a Langmuir−Blodgett trough (Nima Technology, 312D) described previously.[13,37] The trough was cleaned and then filled with Millipore Milli-Q water (resistivity 18.2 MΩ cm). Five mL of the freshly prepared AgNWs was precipitated by centrifuging at 3000 rpm for 5 min. One milliliter of *N*,*N*-dimethylformamide (DMF) was added to disperse the AgNWs to form a homogeneous solution at room temperature. After that, a mixture of 1 mL of $CHCl_3$ was added into the as-prepared homogeneous solution. After that, AgNWs were dispensed onto the water subphase from a 50 μL syringe drop by drop. Thirty minutes later, after spreading, the nanowires surface layer was then compressed with a compression rate of 20 cm^2 min^{-1}. All nanowire films were deposited onto the substrates by the horizontal dipping technique while the constant surface pressure was kept constant as soon as the fold formation that paralleled to the barrier direction occurred.

Synthesis of Cu_2ZnSnS_4 Nanocrystals. Uniform Cu_2ZnSnS_4 nanocrystals were synthesized by a procedure reported previously.[29] In a typical synthesis, 0.130 g of copper(II) acetylacetonate (99.99%, Aldrich), 0.073 g of zinc acetate (99.995%, Aldrich), 0.045 g of $SnCl_2$ (99.99+%, Aldrich), 0.033 g S (99.98%) were mixed with 10 mL of oleylamine (technical grade, Aldrich) and then added into a 25 mL three neck flask connected to a Schlenk line. After degassed vacuum for 30 min and purged with N_2, the mixture is heated to ∼110 °C for 30 min, and turns into a brownish colored solution. The temperature is then raised to 280 °C for 1 h, and then cooled to room temperature. The nanocrystals were then isolated by precipitation with hexane followed by centrifugation.

Characterization. Field-emission scanning electron microscopy (FESEM) was carried out with a field-emission scanning electron microanalyzer (Zeiss Supra 40 scanning eletron microscope at an acceleration voltage of 5 kV.) Transmission electron microscopy (TEM) was carried out on a commercial JEOL-7650 transmission electron microscope operated at an accelerating voltage of 100 kV. The phase purity of the as-prepared products was determined by X-ray diffraction (XRD) using a Philips X'Pert Pro Super X-ray diffractometer equipped with graphite-monochromatized Cu KR radiation. Raman scattering spectra

were recorded with a JY LabRam HR 800 using the 514 nm line of Ar+ for excitation. Innova 40 Benchtop Incubator Shaker was used for the chemical transformation reactions. UV−vis spectra were recorded on a UV-2501PC/2550 at room temperature (Shimadzu Corporation, Japan).

Conflict of Interest: The authors declare no competing financial interest.

Acknowledgment. S.H.Y. acknowledge the funding support from the National Basic Research Program of China (Grant 2010CB934700), the National Natural Science Foundation of China (Grants 91022032, 21061160492, J1030412), Chinese Academy of Sciences (Grant KJZD-EW-M01-1), International Science & Technology Cooperation Program of China (Grant 2010DFA41170), and the Principal Investigator Award by the National Synchrotron Radiation Laboratory at the University of Science and Technology of China (USTC). J. W. Liu thanks the USTC Special Grant for Postgraduate Research, Innovation and Practice and CAS Special Grant for Postgraduate Research, Innovation and Practice, the Fundamental Research Funds for the Central Universities (WK 2340000033). We are grateful for the useful talks with Dr. Xiao-Ming Feng and Tan-Wei Li about the TEM measurement.

Supporting Information Available: Field-emission scanning electron microscopy (FESEM) image of a Cu grid, XRD diffraction patterns and of the Te nanowires, Cu_2ZnSnS_4 nanoparticles, Ag nanowires, and graphene. Raman scattering spectrum of the graphene. UV−vis absorption spectra of the Au nanorods. This material is available free of charge *via* the Internet at http://pubs.acs.org.

REFERENCES AND NOTES

1. Scholes, G. D.; Rumbles, G. , Excitons in Nanoscale Systems. *Nat. Mater.* **2006**, *5*, 683–696.
2. Michalet, X.; Pinaud, F. F.; Bentolila, L. A.; Tsay, J. M.; Doose, S.; Li, J. J.; Sundaresan, G.; Wu, A. M.; Gambhir, S. S.; Weiss, S. Quantum Dots for Live Cells, *in Vivo* Imaging, and Diagnostics. *Science* **2005**, *307*, 538–544.
3. Daniel, M. C.; Astruc, D. Gold Nanoparticles: Assembly, Supramolecular Chemistry, Quantum-Size-Related Properties, and Applications toward Biology, Catalysis, and Nanotechnology. *Chem. Rev.* **2003**, *104*, 293–346.
4. Gates, B. D.; Xu, Q.; Stewart, M.; Ryan, D.; Willson, C. G.; Whitesides, G. M. New Approaches to Nanofabrication: Molding, Printing, and Other Techniques. *Chem. Rev.* **2005**, *105*, 1171–1196.
5. Overgaag, K.; Evers, W.; de Nijs, B.; Koole, R.; Meeldijk, J.; Vanmaekelbergh, D. Binary Superlattices of PbSe and CdSe Nanocrystals. *J. Am. Chem. Soc.* **2008**, *130*, 7833–7835.
6. Urban, J. J.; Talapin, D. V.; Shevchenko, E. V.; Kagan, C. R.; Murray, C. B. Synergismin Binary Nanocrystal Superlattices Leads to Enhanced p-Type Conductivity in Self-Assembled PbTe/Ag_2Te Thin Films. *Nat. Mater.* **2007**, *6*, 115–121.
7. Shevchenko, E. V.; Talapin, D. V.; Kotov, N. A.; O'Brien, S.; Murray, C. B. Structural Diversity in Binary Nanoparticle Superlattices. *Nature* **2006**, *439*, 55–59.
8. Kalsin, A. M.; Fialkowski, M.; Paszewski, M.; Smoukov, S. K.; Bishop, K. J. M.; Grzybowski, B. A. Electrostatic Self-Assembly of Binary Nanoparticle Crystals with a Diamond-like Lattice. *Science* **2006**, *312*, 420–424.
9. Peng, H. S.; Sun, X. M.; Cai, F. J.; Chen, X. L.; Zhu, Y. C.; Liao, G. P.; Chen, D. Y.; Li, Q. W.; Lu, Y. F.; Zhu, Y. T.; *et al.* Electrochromatic Carbon Nanotube/Polydiacetylene Nanocomposite Fibres. *Nat. Nanotechnol.* **2009**, *4*, 738–741.
10. Song, G. T.; Chen, C.; Qu, X. G.; Miyoshi, D.; Ren, J. S.; Sugimoto, N. Small-Molecule-Directed Assembly: A Gold Nanoparticle-Based Strategy for Screening of Homo-adenine DNA Duplex Binders. *Adv. Mater.* **2008**, *20*, 706–710.
11. Zhao, Y.; Thorkelsson, K.; Mastroianni, A. J.; Schilling, T.; Luther, J. M.; Rancatore, B. J.; Matsunaga, K.; Jinnai, H.; Wu, Y.; Poulsen, D.; *et al.* Small-Molecule-Directed Nanoparticle Assembly towards Stimuli-Responsive Nanocomposites. *Nat. Mater.* **2009**, *8*, 979–985.
12. Yao, H. B.; Fang, H. Y.; Tan, Z. H.; Wu, L. H.; Yu, S. H. Biologically Inspired, Strong, Transparent, and Functional Layered Organic−Inorganic Hybrid Films. *Angew. Chem., Int. Ed.* **2010**, *49*, 2140–2145.
13. Liu, J. W.; Zhu, J. H.; Zhang, C. L.; Liang, H. W.; Yu, S. H. Mesostructured Assemblies of Ultrathin Superlong Tellurium Nanowires and Their Photoconductivity. *J. Am. Chem. Soc.* **2010**, *132*, 8945–8952.
14. Srivastava, S.; Kotov, N. A. Composite Layer-by-Layer (LBL) Assembly with Inorganic Nanoparticles and Nanowires. *Acc. Chem. Res.* **2008**, *41*, 1831–1841.
15. Hu, M. J.; Lu, Y.; Zhang, S.; Guo, S. R.; Lin, B.; Zhang, M.; Yu, S. H. High Yield Synthesis of Bracelet-like Hydrophilic Ni−Co Magnetic Alloy Flux-Closure Nanorings. *J. Am. Chem. Soc.* **2008**, *130*, 11606–11607.
16. Shi, H. Y.; Hu, B.; Yu, X. C.; Zhao, R. L.; Ren, X. F.; Liu, S. L.; Liu, J. W.; Feng, M.; Xu, A. W.; Yu, S. H. Ordering of Disordered Nanowires: Spontaneous Formation of Highly Aligned, Ultralong Ag Nanowire Films at Oil−Water−Air Interface. *Adv. Funct. Mater.* **2010**, *20*, 958–964.
17. Maheshwari, S.; Zhang, L.; Zhu, Y.; Chang, H. C. Coupling Between Precipitation and Contact-Line Dynamics: Multiring Stains and Stick-Slip Motion. *Phys. Rev. Lett.* **2008**, *100*, 044503.
18. Ming, T.; Kou, X.; Chen, H.; Wang, T.; Tam, H. L.; Cheah, K. W.; Chen, J. Y.; Wang, J. Ordered Gold Nanostructure Assemblies Formed By Droplet Evaporation. *Angew. Chem., Int. Ed.* **2008**, *47*, 9685–9690.
19. Fava, D.; Winnik, M. A.; Kumacheva, E. Photothermally-Triggered Self-Assembly of Gold Nanorods. *Chem. Commun.* **2009**, 2571–2573.
20. Zhou, J. F.; Sedev, R.; Beattie, D.; Ralston, J. Light-Induced Aggregation of Colloidal Gold Nanoparticles Capped by Thymine Derivatives. *Langmuir* **2008**, *24*, 4506–4511.
21. Kim, W. J.; Kim, S. J.; Lee, K. S.; Samoc, M.; Cartwright, A. N.; Prasad, P. N. Robust Microstructures Using UV Photopatternable Semiconductor Nanocrystals. *Nano Lett.* **2008**, *8*, 3262–3265.
22. Smith, A. R.; Watson, D. F. Photochemically Triggered Assembly of Composite Nanomaterials through the Photodimerization of Adsorbed Anthracene Derivatives. *Chem. Mater.* **2010**, *22*, 294–304.
23. Qi, X.; Huang, Y.; Klapper, M.; Boey, F.; Huang, W.; Feyter, S. D.; Müllen, K.; Zhang, H. *In Situ* Modification of Three-Dimensional Polyphenylene Dendrimer-Templated CuO Rice-Shaped Architectures with Electron Beam Irradiation. *J. Phys. Chem. C* **2010**, *114*, 13465–13470.
24. Son, J. G.; Chang, J. B.; Berggren, K. K.; Ross, C. A. Assembly of Sub-10-nm Block Copolymer Patterns with Mixed Morphology and Period Using Electron Irradiation and Solvent Annealing. *Nano Lett.* **2011**, *11*, 5079–5084.
25. Warner, J. H. Self-Assembly of Ligand-Free PbS Nanocrystals into Nanorods and Their Nanosculpturing by Electron-Beam Irradiation. *Adv. Mater.* **2008**, *20*, 784–787.
26. de Jonge, N.; Ross, F. M. Electron Microscopy of Specimens in Liquid. *Nat. Nanotechnol.* **2011**, *6*, 695–704.
27. Zheng, H.; Smith, R. K.; Jun, Y.-w.; Kisielowski, C.; Dahmen, U.; Alivisatos, A. P. Observation of Single Colloidal Platinum Nanocrystal Growth Trajectories. *Science* **2009**, *324*, 1309–1312.
28. Dong, Z.; Lai, X.; Halpert, J. E.; Yang, N.; Yi, L.; Zhai, J.; Wang, D.; Tang, Z.; Jiang, L. Accurate Control of Multishelled ZnO Hollow Microspheres for Dye-Sensitized Solar Cells with High Efficiency. *Adv. Mater.* **2012**, *24*, 1046–1049.
29. Steinhagen, C.; Panthani, M. G.; Akhavan, V.; Goodfellow, B.; Koo, B.; Korgel, B. A. Synthesis of Cu_2ZnSnS_4 Nanocrystals for Use in Low-Cost Photovoltaics. *J. Am. Chem. Soc.* **2009**, *131*, 12554–12555.
30. Xiao, M.; Chen, H. J.; Ming, T.; Shao, L.; Wang, J. F. Plasmon-Modulated Light Scattering from Gold Nanocrystal-Decorated Hollow Mesoporous Silica Microspheres. *ACS Nano* **2010**, *4*, 6565–6572.
31. Yang, C.; Gu, H. W.; Lin, W.; Yuen, M. M.; Wong, C. P.; Xiong, M. Y.; Gao, B. Silver Nanowires: From Scalable Synthesis to Recyclable Foldable Electronics. *Adv. Mater.* **2011**, *23*, 3052–3056.

32. Qian, H. S.; Yu, S. H.; Gong, J. Y.; Luo, L. B.; Fei, L. F. High-Quality Luminescent Tellurium Nanowires of Several Nanometers in Diameter and High Aspect Ratio Synthesized by a Poly (vinyl pyrrolidone)-Assisted Hydrothermal Process. *Langmuir* **2006**, *22*, 3830–3835.
33. Xu, Y. X.; Bai, H.; Lu, G. W.; Li, C.; Shi, G. Q. Flexible Graphene Films *via* the Filtration of Water-Soluble Noncovalent Functionalized Graphene Sheets. *J. Am. Chem. Soc.* **2008**, *130*, 5856–5857.
34. Hummers, W. S.; Offeman, R. E. Preparation of Graphitic Oxide. *J. Am. Chem. Soc.* **1958**, *80*, 1339–1339.
35. Tung, V. C.; Allen, M. J.; Yang, Y.; Kaner, R. B. High-Throughput Solution Processing of Large-Scale Graphene. *Nat. Nanotechnol.* **2009**, *4*, 25–29.
36. Most samples for transmission electron microscopy must be "supported" on some kind of a thin electron transparent film, to hold the specimen in place while in the objective lens of the TEM. Thin carbon film is the most common support films for TEM grids, and the thickness of carbon film is around 10 nm.
37. Tao, A.; Kim, F.; Hess, C.; Goldberger, J.; He, R. R.; Sun, Y. G.; Xia, Y. N.; Yang, P. D. Langmuir−Blodgett Silver Nanowire Monolayers for Molecular Sensing Using Surface-Enhanced Raman Spectroscopy. *Nano Lett.* **2003**, *3*, 1229–1233.
38. Yu, D.; Liu, F. Synthesis of Carbon Nanotubes by Rolling up Patterned Graphene Nanoribbons Using Selective Atomic Adsorption. *Nano Lett.* **2007**, *7*, 3046–3050.
39. Guo, X. Y.; Li, H.; Ahn, B. Y.; Duoss, E. B.; Hsia, K. J.; Lewis, J. A.; Nuzzo, R. G. Two- and Three-Dimensional Folding of Thin Film Single-Crystalline Silicon for Photovoltaic Power Applications. *Proc. Natl. Acad. Sci. U.S.A.* **2009**, *106*, 20149–20154.
40. Schmidt, O. G.; Eberl, K. Nanotechnology—Thin Solid Films Roll up into Nanotubes. *Nature* **2001**, *410*, 168–168.
41. Shenoy, V. B.; Reddy, C. D.; Zhang, Y. W. Spontaneous Curling of Graphene Sheets with Reconstructed Edges. *ACS Nano* **2010**, *4*, 4840–4844.
42. Schmidt, O. G.; Schmarje, N.; Deneke, C.; Muller, C.; Jin-Phillipp, N. Y. Three-Dimensional Nano-objects Evolving from a Two-Dimensional Layer Technology. *Adv. Mater.* **2001**, *13*, 756–759.
43. Mei, Y. F.; Thurmer, D. J.; Deneke, C.; Kiravittaya, S.; Chen, Y. F.; Dadgar, A.; Bertram, F.; Bastek, B.; Krost, A.; Christen, J.; *et al*. Fabrication, Self-Assembly, and Properties of Ultrathin AlN/GaN Porous Crystalline Nanomembranes: Tubes, Spirals, and Curved Sheets. *ACS Nano* **2009**, *3*, 1663–1668.
44. Cho, J. H.; James, T.; Gracias, D. H. Curving Nanostructures Using Extrinsic Stress. *Adv. Mater.* **2010**, *22*, 2320–2324.
45. Guo, X. H.; Yu, S. H.; Lu, Y.; Yuan, G. B.; Sedlak, M.; Colfen, H. Spontaneous Formation of Hierarchically Structured Curly Films of Nickel Carbonate Hydrate through Drying. *Langmuir* **2010**, *26*, 10102–10110.
46. Stoney, G. G. The Tension of Metallic Films Deposited by Electrolysis. *Proc. R. Soc., London., Ser. A* **1909**, *82*, 172–175.
47. Banhart, F. Irradiation of Carbon Nanotubes with a Focused Electron Beam in the Electron Microscope. *J. Mater. Sci.* **2006**, *41*, 4505–4511.
48. Banhart, F. Irradiation Effects in Carbon Nanostructures. *Rep. Prog. Phys.* **1999**, *62*, 1181–1221.
49. Ugarte, D. Curling and Closure of Graphitic Networks under Electron-Beam Irradiation. *Nature* **1992**, *359*, 707–709.
50. Nikishkov, G. P. Curvature Estimation for Multilayer Hinged Structures with Initial Strains. *J. Appl. Phys.* **2003**, *94*, 5333–5336.
51. Cendula, P.; Kiravittaya, S.; Mei, Y. F.; Deneke, C.; Schmidt, O. G. Bending and Wrinkling as Competing Relaxation Pathways for Strained Free-Hanging Films. *Phys. Rev. B* **2009**, *79*, 085429.